

# Contingent Nonlinear Model Predictive Control for Collision Imminent Steering in Uncertain Environments

James Dallas, John Wurts, Jeffrey L. Stein, Tulga Ersal\*\*

Department of Mechanical Engineering, University of Michigan, Ann Arbor, MI 48109.

\*\* Corresponding author: [tersal@umich.edu](mailto:tersal@umich.edu)

---

**Abstract:** A novel uncertainty based contingent model predictive control algorithm is presented for autonomous vehicles operating in uncertain environments. Nominal model predictive control relies on a model to predict future states over a horizon and hence requires accurate models and parameterization. In application, environmental conditions and parameters may be unknown or varying, posing robustness issues for model predictive control. This work presents a new selectively robust adaptive model predictive control algorithm that is applied to collision imminent steering controllers for automotive safety. In this context, uncertainties in the road coefficient of friction are estimated using unscented Kalman filtering and the controller is updated based upon the estimated uncertainties. The utility of the uncertainty based controller is demonstrated in a collision imminent steering scenario and compared to nominal deterministic model predictive control, as well as a baseline adaptive scheme. The results suggest the uncertainty based controller can improve the robustness of model predictive control by nearly 50% for deterministic model predictive control and over 10% for the baseline adaptive scheme.

*Keywords:* Automotive control, nonlinear predictive control, adaptive control, robust control, parameter estimation, Kalman filtering

---

## 1. INTRODUCTION

Recently, the advancement of active safety features have drawn interest to assist human drivers in safety critical scenarios, for example in the case of collision imminent steering (CIS), e.g., Wurts et al. (2018, 2019). In such a scenario, a vehicle is forced to perform immediate evasive steering to avoid a forward collision where braking alone is insufficient due to the close proximity of an obstacle. Due to the aggressive nature of this maneuver, the vehicle is often pushed near its handling limits, requiring accurate modeling of the vehicle's nonlinearities and hence a nonlinear control formulation.

Model predictive control (MPC) has drawn interest in such applications, as it allows for one to formally and explicitly implement safety constraints and vehicle dynamics, e.g., Liu et al. (2017); Anderson et al. (2010); Chakraborty et al. (2013); Schwarting et al. (2017); Brown et al. (2017). However, such approaches often rely on exact knowledge of the system and environment parameters and may not be suitable for situations where the environment is only partially known, such as when road conditions are unknown *a priori*, e.g., Wurts et al. (2019); Liu et al. (2017); Laurence et al. (2017). Such a scenario is likely to occur in practice, for example when the road friction is reduced due to weather or road surface changes. While the feedback and controller update of MPC inherently provides a level of robustness in terms of model discrepancy, large uncertainties in models can still lead to failure, e.g., Liu et al.

(2016, 2019). In fact, due to the sensitivity of tire models to the coefficient of friction, a deviation of just 2% can lead to failure in certain scenarios, e.g., Laurence et al. (2017). Conservative formulations can offer robustness, but at the expense of performance, e.g., Liu et al. (2019). As such, being able to learn these model uncertainties and adapt the controller in real-time is critical in safely transitioning autonomous features from controlled and known experimental situations to real world applications.

To address this need, researchers have considered estimating the coefficient of friction and updating control strategies online, e.g., Chen et al. (2014); Ji et al. (2018); Falcone et al. (2007); Borrelli et al. (2005). Chen et al. (2014) utilized MPC with a linear time-varying vehicle model for the design of a lane keeping system. Ji et al. (2018) utilized a cornering stiffness based model for lateral motion control and path tracking. Finally, Falcone et al. (2007) used a nonlinear vehicle model with Pacejka tire models in nonlinear MPC (NMPC); however, due to high computational costs, the model is only suitable for low speed operation and a linearized model is utilized for high speed operation. Further, Falcone et al. (2007) assume a trajectory is known *a priori* and employ MPC in an attempt to follow the trajectory. A similar study was also reported by Borrelli et al. (2005).

While the results of these studies are promising, two limitations of them must be considered when vehicles are operating at high speeds and are pushed near their handling limits. First, linearization can lead to large discrepancies between the control model and the physical system, which poses safety issues, especially considering the high speeds and aggressive nature of CIS maneuvers, e.g., Liu et al. (2017); Wurts et al. (2019). Second, if the trajectory plan-

---

<sup>1</sup> Toyota Research Institute ("TRI") provided funds to assist the authors with their research, but this article solely reflects the opinions and conclusions of the authors and not TRI or any other Toyota entity.

ning and trajectory tracking problems are decoupled as in these studies, safety issues may arise in CIS, where the vehicle is operating near its handling limits. This results from the fact that without a complete understanding of the vehicle's handling limits, planners can generate reference trajectories that the vehicle may not be able to follow no matter how sophisticated the trajectory trackers may be.

Alsterda et al. (2019) address the problem of operating on unknown road conditions by using contingent MPC (CMPC), a selectively robust MPC formulation designed to address the conservative nature of robust MPC (RMPC). In this approach, two separate predictions are solved by MPC simultaneously; a nominal and a contingent prediction. The objective is to find a feasible control such that the initial control move of the nominal and contingent models are consistent. In this way, it was demonstrated that contingent MPC can outperform deterministic MPC when preparing for an ice covered terrain instead of snow. While this approach proposes a method for planning for these discrete scenarios, additional robustness could be achieved by not necessarily planning for two separate scenarios, but by learning about the coefficient of friction online and exploiting the uncertainty of the learned parameter in a similar manner as contingent MPC.

Based upon this review, it is evident that a gap exists in learning the road conditions online and incorporating these observations in a control architecture suitable for scenarios where vehicles are operating near their handling limits. To this extent, the contribution of this work is the development of an uncertainty based contingency MPC formulation for CIS under uncertain road conditions. While this article focuses specifically on the CIS application, the approach could be applied to off-road autonomous vehicles and a more general class of systems where real time decision-making is influenced by an unknown environment.

The remainder of this paper is organized as follows. In Sec. 2 the CIS problem, vehicle modeling, friction estimation, and uncertainty based contingent MPC are presented. In Sec. 3, the impact of uncertain road conditions on controller error are presented along with the integration of friction estimation to mitigate these resulting errors. Sec. 4 discusses the utility of the uncertainty based contingent MPC formulation. Finally, Sec. 5 draws the concluding remarks of this study.

## 2. PROBLEM FORMULATION

### 2.1 Collision Imminent Steering

The CIS scenario occurs in high speed applications, for example highway operation, and begins with a vehicle centered in the right lane of a right hand curved highway and travelling at 35 m/s. At time  $t_0$  the vehicle identifies an obstruction in the right lane 55 m ahead. Due to the high speed of the vehicle, there is insufficient time for the vehicle to brake to prevent collision, which requires a 62.4 m lead at a peak deceleration of  $1g$ , where  $g$  is the gravitational acceleration. As such, the vehicle must perform an emergency lane change into the left lane to prevent collision. For the purposes of this work, the maneuver is considered safe if the vehicle (i) avoids collision with the obstacle, (ii) does not violate the outside lane boundaries, and (iii) settles in the center of the left lane. Due to the aggressive nature of this maneuver, the controller forces the vehicle to operate near its handling

limits, see Wurts et al. (2018). Further information on CIS can be found in Wurts et al. (2019).

### 2.2 Vehicle Models

This work utilizes two vehicle models; a 14 degree-of-freedom (DoF) vehicle model representing the plant and a 3 DoF bicycle model for predictions in the unscented Kalman filter (UKF) and MPC framework.

In this work, the 14 DoF model represents the ground truth. Details on the 14 DoF model can be found in Shim and Ghike (2007).

For the vehicle trajectory predictions in MPC and the UKF, the prediction model is represented as a 3 DoF bicycle model, as this has shown to be of a proper balance between level of fidelity and efficiency for short-horizon predictions, e.g., Liu et al. (2016); Dallas et al. (2020). The bicycle model is given as

$$\dot{\mathbf{z}}(\mu^*) = \begin{bmatrix} u \cos \psi - v \sin \psi \\ u \sin \psi + v \cos \psi \\ w_z \\ 0 \\ (F_{yf}(\mu^*) \cos(\delta_f) + F_{yr}(\mu^*)/M_t - u\omega_z) \\ (F_{yf}(\mu^*) \cos(\delta_f)L_f - F_{yr}(\mu^*)L_r)/I_{zz} \\ \delta_f \end{bmatrix} \quad (1)$$

where the state vector,  $\mathbf{z}$ , is defined as

$$\mathbf{z} := \begin{bmatrix} x \\ y \\ \psi \\ u \\ v \\ \omega_z \\ \delta_f \end{bmatrix} = \begin{bmatrix} \text{global } x \text{ position of CoM} \\ \text{global } y \text{ position of CoM} \\ \text{yaw angle} \\ \text{longitudinal velocity} \\ \text{lateral velocity} \\ \text{yaw rate} \\ \text{front steering angle} \end{bmatrix} \quad (2)$$

and  $\mu^*$  is the road coefficient of friction,  $M_t$  is the vehicle mass,  $I_{zz}$  is the vehicle's yaw moment of inertia, and  $L_f$  and  $L_r$  are the distances from the vehicle's center of mass (CoM) to the front and rear axles, respectively. Finally, the tire lateral forces,  $F_{yf}$  and  $F_{yr}$ , are given by the nonlinear Pacejka formula

$$F_y(\mu^*) = -\mu^* F_z \sin \left( C \arctan \left( B \frac{V_x}{V_y} \right) \right) \quad (3)$$

where  $V_x$  and  $V_y$  are the tire patch velocities in the longitudinal and lateral directions,  $F_z$  is the normal load on the tire, and  $B$  and  $C$  are Pacejka curve parameters, see Pacejka (2006).

### 2.3 Coefficient of Friction Estimation

To estimate the coefficient of friction, a UKF is utilized as described in Dallas et al. (2020), but with the prediction model given by the bicycle model and Pacejka tire model of Eqs. (1)-(3). To achieve the UKF prediction model format of Dallas et al. (2020), the bicycle model of Eq. (1) is appended with an additional state representing the coefficient of friction with trivial dynamics. The UKF utilizes this model in a predictor-corrector scheme, where (i) predictions are performed by the 3 DoF bicycle model appended with the coefficient of friction, and (ii) correction is performed based upon measurements of the vehicle states. The UKF then determines the best estimate based upon the uncertainties of the measurements and the 3 DoF bicycle model. In this work, vehicle state measurements are obtained by corrupting the 14 DoF model with Gaussian noise of standard deviations given in Table 1.

Table 1. Measurement standard deviations used for sensor simulation.

State	Noise ( $\sigma$ )
$x$	1.2 (m)
$y$	1.2 (m)
$\psi$	0.0175 (rad)
$u$	0.25 (m/s)
$v$	0.25 (m/s)
$\omega_z$	0.0175 (rad/s)

The sensor noise is higher than typically reported, e.g. (Ryu et al., 2002), and hence acts as a worst-case scenario. Furthermore, the scenario assumes a discrete change in the coefficient of friction at  $t_0$ , acting in a worst-case manner. A more detailed explanation of the UKF is given in Wan and Van Der Merwe (2000); Kolås et al. (2009). Although many other estimation techniques are available, the UKF is used in this work, because it was found to offer a suitable balance between computational efficiency and estimation accuracy, see Dallas et al. (2020).

#### 2.4 Model Predictive Control Formulation

The nonlinear MPC formulation extends upon Wurts et al. (2019), which also serves as the nominal deterministic MPC formulation for benchmarking purposes. Briefly, the formulation is designed to minimize the peak tire slip, thereby minimizing the aggressiveness of the maneuver while maximizing available control authority. A more detailed explanation can be found in Wurts et al. (2019). To map the control inputs to future vehicle states, the RK4 integration scheme is applied to an augmented vector of Eq. (1) to apply contingent MPC. Thus, the augmented dynamics become

$$\dot{\mathbf{z}}_{\mathbf{c}}(\mu^*) = \begin{bmatrix} \dot{z}(\mu_1) \\ \dot{z}(\mu_2) \end{bmatrix} \quad (4)$$

with the control input,  $\mathbf{u}$ , being

$$\mathbf{u} = \begin{bmatrix} u^{\mu_1} \\ u^{\mu_2} \end{bmatrix} = \begin{bmatrix} \delta_f^{\mu_1} \\ \delta_f^{\mu_2} \end{bmatrix} \quad (5)$$

with  $\delta_f$  being the steering rate of the front tires and  $\mu_1$  and  $\mu_2$  representing lower and upper bounds on the confidence interval of the estimate of the coefficient of friction, respectively. For this work, one, two, and three standard deviation bounds are analyzed, which are reported to MPC by the UKF at each new MPC iteration. The nominal deterministic formulation is then extended to a contingent MPC formulation as follows.

$$\begin{aligned} \min_{\mathbf{u}} \quad & (u_1^{\mu_1} - u_1^{\mu_2})^2 + \frac{1}{\rho_{\text{obj}}} \ln \sum_{i=1}^n e^{\rho_{\text{obj}} |\alpha_i^{\mu_1}|} \\ \text{subject to} \quad & \begin{bmatrix} d_i^{\text{left edge}} \\ d_i^{\text{right edge}} \\ |\alpha_{f,i}| - \alpha^{\text{peak}} \\ |\alpha_{r,i}| - \alpha^{\text{peak}} \\ |\delta_f(t_i)| - \delta_f^{\text{max}} \\ |\dot{\delta}_f(t_i)| - \dot{\delta}_f^{\text{max}} \end{bmatrix} \leq 0 \quad \forall i \in [1, n] \\ & (\mathbf{x}_t)_i - (\mathbf{x}_{\text{stable}})_i = 0 \quad \forall i \in [4, 7] \\ & (x_t - x_c)^2 + (y_t - y_c)^2 = r_{\text{lane}}^2 \\ & \arctan\left(\frac{y_t - y_c}{x_t - x_c}\right) = \frac{\pi}{2} - \arctan\left(\frac{v_t}{u_0}\right) \end{aligned} \quad (6)$$

where  $\rho_{\text{obj}}$  is the constraint aggregation parameter,  $d^{\cdot \text{edge}}$  are distances to the edges of the drivable tube,  $\alpha_{f,r}$  are the

tire slip angles at the front and rear tires,  $\alpha^{\text{peak}}$  is the peak slip angle constraint, and  $\delta_f^{\text{max}}$  and  $\dot{\delta}_f^{\text{max}}$  are constraints on the maximum steering angle and steering rate of the front tires. Finally,  $\mathbf{x}_t$  represents the terminal state,  $(x_c, y_c)$  represents the terminal road arc position,  $r_{\text{lane}}$  is the lane radius of curvature, and  $\mathbf{x}_{\text{stable}}$  is the terminal constraint on the last four states of Eq. (2).

The equality and inequality constraints maintain consistency with Wurts et al. (2019), and the detailed descriptions can be found therein. However, there are several differences in the formulation of the cost function of Eq. (6). First, the contribution of the peak tire slip to the cost is only calculated for the lower bound of the coefficient of friction,  $\mu_1$ . This is because the lower coefficient of friction makes it harder for the vehicle to induce the lateral force necessary to satisfy the problem constraints, hence forcing a larger slip angle, effectively pushing the vehicle towards its handling limits. Second, an additional cost is added to attempt to force the first control moves of the two contingency models to be equal. Here it is suggested that only the first control move of each contingency model be equal, as only the initial control move is applied and future control inputs are discarded in the next MPC iteration. In the case that  $u_1^{\mu_1}$  and  $u_1^{\mu_2}$  are not equal, an average of the two is sent to the controller, as this represents the current best estimate of  $\mu$ . This situation would occur if the vehicle is quite close to the obstacle and the constraints are active for both contingency models. For this work, a 3.2 s time horizon with 50 ms discretization time step is used to represent current automotive architectures. Hence a zero order hold is placed on the first control move that is sent to the plant. Finally, the equality and inequality constraints are applied to relevant variables of both contingency models.

The optimal control problem (OCP) of Eq. (6) is solved through IPOPT (see Wächter and Biegler (2006)) and the trajectory is simulated using multiple shooting on a custom CUDA implementation. Within each segment, the system dynamics of Eq. (1) are numerically simulated using RK4 integration, directly accounting for the system dynamic constraints as in Wurts et al. (2019). The peak computation time of the UKF is less than 770  $\mu\text{s}$ . The CUDA wall time is 800  $\mu\text{s}$  and the total wall time is between 80 ms and 4 s on an Intel-i7 CPU and NVidia GTX 1080 GPU. In comparison, the nonadaptive deterministic and baseline adaptive MPC have a peak wall time of 55 ms. However, it is worth noting that the total wall time is approximately 99% solve time in IPOPT versus 1% wall time simulating the contingent trajectories for fitness and feasibility. Introducing the contingency between the two models adds significant cross sensitivity in the optimization problem, which could feasibly be addressed by a more efficient solver.

### 3. MPC PREDICTION ERROR AND INTEGRATION OF UKF

#### 3.1 MPC Prediction Error

The uncertainty of the coefficient of friction manifests in MPC error due to the inaccuracies of the resulting bicycle model predictions over the horizon. A misrepresentation of the coefficient of friction can result in two conditions: the plant is over-responsive or under-responsive. When the predicted coefficient of friction is lower than the true plant value, the plant is over-responsive and results in

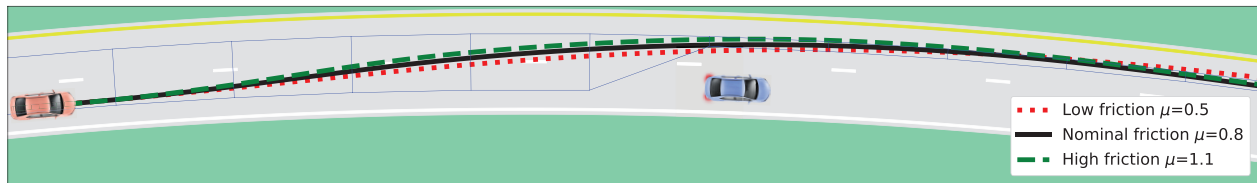


Fig. 1. Open loop trajectory for low coefficient of friction (red dotted line), nominal (black solid line), and high coefficient of friction (green dashed line) under the same control inputs. Blue lines represent the safe drivable tube.

more aggressive turns than intended by the controller. This can result in overturning into the obstacle when the controller attempts to turn in avoidance of the outer lane boundary. In the case that the predicted coefficient of friction is larger than the true plant value, the plant is under-responsive and reacts by less aggressive turning than intended by the controller. This results in failure, since the vehicle drifts outside of the outer lane boundary instead of correctly counter-steering back towards the inside of the turn. This under-responsive case is the focus of this work and correlates to the scenario of a vehicle suddenly encountering degraded road conditions in terms of reduced friction, such as a patch of ice or snow.

To demonstrate these MPC errors, the impact of the coefficient of friction is depicted in Fig. 1 for a low coefficient of friction (red dotted line), a nominal value (black solid line), and a high coefficient of friction (green dashed line) under the same open-loop control input. As such, the proposed CMPC attempts to address this scenario by finding a feasible solution through estimating both lower and upper bounds on the confidence interval of the coefficient of friction estimate. By doing so, the impact of prediction error is minimized such that the CIS maneuver can be completed in a safe manner, as described in Sec. 2.1. This applies a more conservative adaptation to the road conditions than directly utilizing the current best estimate of the coefficient of friction.

### 3.2 Friction Estimator and MPC Integration

To address the prediction error described in Sec. 3.1, the UKF estimator is implemented to run in parallel with contingent MPC as follows. First, the UKF is running at a 1 kHz prediction rate with a 50 Hz measurement update, received from the noise-corrupted plant states. This update rate is selected to be comparable to standard sensors. At the initial time,  $t_0$ , in each MPC iteration, the UKF sends CMPC the current estimate of the coefficient of friction and the standard deviation of the estimate obtained from the UKF state covariance matrix. From this data,  $\mu_1$  and  $\mu_2$  are calculated as required by CMPC. CMPC then solves for the optimal control input sequence for the entire prediction horizon by assuming  $\mu_1$  and  $\mu_2$  are held constant. The first control move generated by the OCP is sent to the plant. While the OCP is being solved, the UKF is running independently. This process is then repeated such that at the initialization of the next CMPC iteration, the UKF reports the current coefficient of friction estimate and its standard deviation corresponding to the shifted  $t_0$ .

## 4. RESULTS AND DISCUSSION

To assess the utility of the uncertainty based contingent MPC, CIS simulations are run for various controller cases.

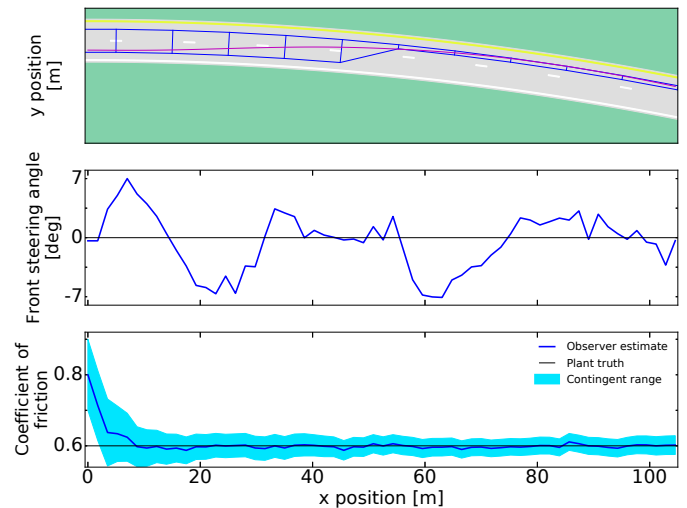


Fig. 2. Sample CIS maneuver for under-responsive initialization. Top plot shows the vehicle trajectory (red), middle plot shows the steering profile of the maneuver, and bottom plot depicts the estimator performance (solid blue line) and contingency range (shaded cyan region).

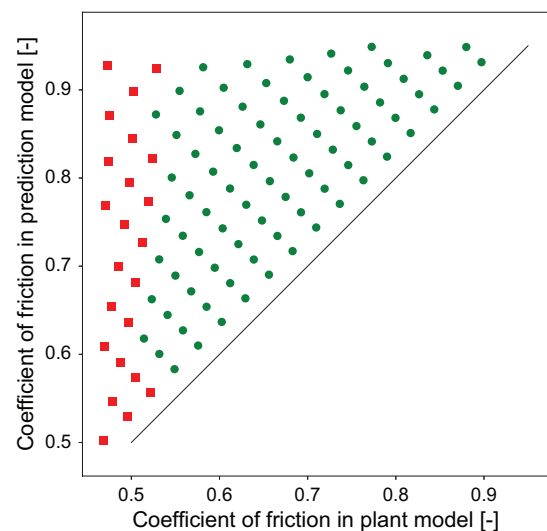


Fig. 3. Various initializations of coefficient of friction for  $1\sigma$  uncertainty based MPC simulations. Green dots depict success and red squares demonstrate failure in solving the OCP.

Each simulation initializes the scenario with a separate plant coefficient of friction and initial guess used by the prediction model at the beginning of an event. While the problem is initialized with these coefficients, as the simulation runs the estimator is attempting to determine an estimate of the plant's coefficient of friction.

As an example, Fig. 2 shows profiles of the vehicle's trajectory, steering angle, and estimated coefficient of friction when the initial prediction model guess is 0.8 and the true plant value is 0.6. The top plot depicts the vehicle departing the right lane and successfully avoiding collision (red solid line). The UKF's ability to recover the plant coefficient of friction is depicted in the bottom plot. The estimator initially believes the coefficient to be 0.8, but rapidly converges to within 2% of the true plant value (0.6) in less than 250 ms. Such fast convergence is critical, because prior to estimator convergence, the vehicle may exhibit the over- and under-responsive behaviors mentioned in Sec. 3.1. Hence, the more rapidly the estimator can converge, the earlier corrected control inputs can be applied.

Fig. 3 shows the various under-responsive initializations studied. A distinct region of failure exists around a large success area. In the far left failure region, which occurs at around 0.52 plant coefficient of friction, the plant coefficient of friction is extremely low, thus reducing the vehicle's ability to generate large lateral forces. In this under-responsive scenario, failure occurs in the OCP solver due to the vehicle drifting outside of the lane boundary, as the control inputs fail to produce the required forces for successful counter-steering. At low plant coefficients of friction, below approximately 0.5, the OCP solver fails, as there is no feasible solution even with exact parameterization. This low coefficient of friction is responsible for the failure in the lower region of all points of initial prediction coefficient of friction below approximately 0.55, because the uncertainty based MPC lower bound on the coefficient of friction becomes parameterized with a value less than 0.5, causing the optimizer to fail to find a feasible solution. Finally, a success region exists where the area represents the achievable robustness to initial plant prediction mismatch. In this region, the estimator is able to successfully predict the coefficient of friction to allow for the prediction model to achieve enough accuracy as compared to the plant for a successful maneuver. In particular, the contingency based MPC formulation demonstrates the most improvement in the far left side where the plant coefficient of friction is low (0.52). This improvement becomes evident when the results for the  $1\sigma$  uncertainty based contingent MPC in Fig. 3 are compared to the baseline adaptive MPC case in Fig. 4. Here, the baseline adaptive MPC scheme refers to updating the MPC prediction model with the current best estimate of the coefficient of friction from the estimator, rather than using the uncertainty based formulation. In addition, the results of the nonadaptive deterministic algorithm are shown in Fig. 5. It is observed that the number of successful OCP solves, and thus the algorithm's robustness, is significantly reduced without any adaptation. The increased area of the success region in Fig. 3 compared to the two benchmarks thus depicts the improvement gained by the contingency based MPC formulation.

Table 2 depicts the improvement in terms of success rate for the initial coefficient of friction mismatch. The adaptive schemes (baseline and uncertainty based MPC variations) significantly expand the success region of the CIS maneuver compared to the nonadaptive deterministic scheme. Furthermore,  $1\sigma$  contingency yields the largest success rate for initial mismatch of coefficient of friction between the plant and prediction models, with only about 20% failure. As seen in Fig. 3, the majority of failures occur at low plant coefficient of frictions, where no feasible solution

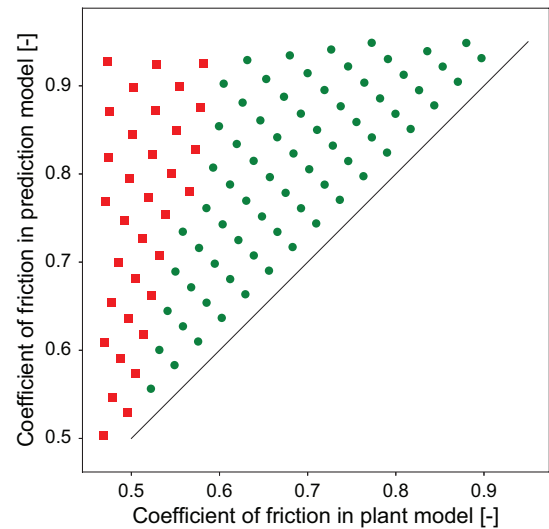


Fig. 4. Various initializations of coefficient of friction for baseline adaptive MPC simulations. Green dots depict success and red squares demonstrate failure in solving the OCP.

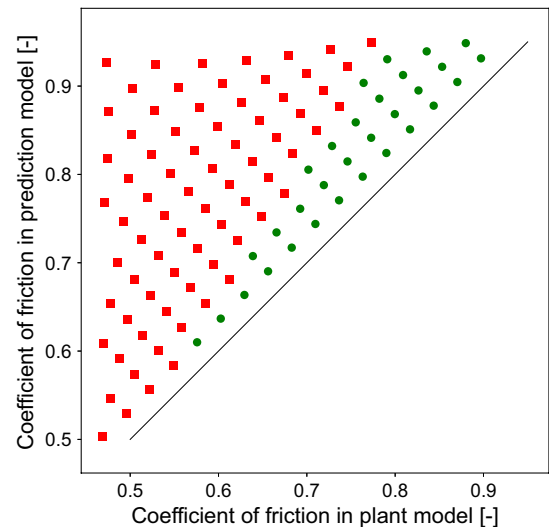


Fig. 5. Various initializations of coefficient of friction for nonadaptive deterministic MPC simulations. Green dots depict success and red squares demonstrate failure in solving the OCP.

exists even with exact parameterization, suggesting the  $1\sigma$  uncertainty based MPC covers the majority of the feasible operation range. At larger uncertainty bounds (2 and  $3\sigma$ ), the uncertainty based contingent MPC formulation becomes too conservative and degrades the performance as compared to smaller uncertainty bounds, because the lower bound prediction model easily becomes parameterized by a low coefficient of friction (0.5), where there is no feasible solution to the problem. Hence, the lower failure region of Fig. 3 is expanded.

These results suggest that uncertainty based contingent MPC can improve robustness in under-responsive operation, for example when the road coefficient is degraded due to moisture or ice, and that adaptive controllers are critical when autonomous vehicles are operating in real world scenarios with only partially known or unknown road conditions. However, it is important to select the uncertainty bounds properly to avoid an overly conservative

Table 2. Success rate under initial coefficient of friction mismatch.

MPC formulation	Success rate
Deterministic	29.2%
Baseline adaptive	67.9%
Uncertainty based MPC $1\sigma$	78.3%
Uncertainty based MPC $2\sigma$	64.1%
Uncertainty based MPC $3\sigma$	48.1%

solution that reduces the robustness benefits of uncertainty based contingent MPC.

## 5. CONCLUSION

This work considers increasing the robustness of autonomous vehicles in CIS applications through adaptation to road conditions. In particular, the coefficient of friction, and its variance, is estimated online by a UKF and integrated into a new single-level uncertainty based contingent MPC for CIS. The uncertainty based contingent MPC seeks to find control moves such that vehicle models parameterized within confidence intervals of the estimate satisfy the problem formulation. Through simulation of a CIS maneuver, it is shown that the developed uncertainty based contingent MPC can outperform deterministic MPC and a baseline adaptive scheme by increasing the initialization error range of the road coefficient of friction for which the OCP can still be successfully solved. Therefore, it is concluded that the developed algorithm could improve the robustness of autonomous vehicles if it can be solved in real time.

Future work should explore various solvers and benchmarking the computational performance for uncertainty based contingent MPC. If real time is achieved by one of these solvers, it is also of interest to perform experimental validation of the proposed scheme.

## REFERENCES

- Alsterda, J., Brown, M., and Gerdes, J.C. (2019). Contingency model predictive control for automated vehicles. In *2019 Annual American Control Conference*, 718–722.
- Anderson, S.J., Peters, S.C., Pilutti, T.E., and Iagnemma, K. (2010). An optimal-control-based framework for trajectory planning, threat assessment, and semi-autonomous control of passenger vehicles in hazard avoidance scenarios. *International Journal of Vehicle Autonomous Systems*, 8(2-4), 190–216.
- Borrelli, F., Falcone, P., Keviczky, T., Asgari, J., and Hrovat, D. (2005). MPC-based approach to active steering for autonomous vehicle systems. *International Journal of Vehicle Autonomous Systems*, 3(2/3/4), 265.
- Brown, M., Funke, J., Erlien, S., and Gerdes, J.C. (2017). Safe driving envelopes for path tracking in autonomous vehicles. *Control Engineering Practice*, 61, 307–316.
- Chakraborty, I., Tsiotras, P., and Diaz, R.S. (2013). Time-optimal vehicle posture control to mitigate unavoidable collisions using conventional control inputs. In *2013 American Control Conference*, 2165–2170.
- Chen, B.C., Luan, B.C., and Lee, K. (2014). Design of lane keeping system using adaptive model predictive control. In *2014 IEEE International Conference on Automation Science and Engineering*, 922–926.
- Dallas, J., Jain, K., Dong, Z., Sapronov, L., Cole, M.P., Jayakumar, P., and Ersal, T. (2020). Online terrain estimation for autonomous vehicles on deformable terrains. *Journal of Terramechanics*, 91, 11 – 22.
- Falcone, P., Borrelli, F., Asgari, J., Tseng, H.E., and Hrovat, D. (2007). Predictive Active Steering Control for Autonomous Vehicle Systems. *IEEE Transactions on Control Systems Technology*, 15(3), 566–580.
- Ji, X., He, X., Lv, C., Liu, Y., and Wu, J. (2018). Adaptive-neural-network-based robust lateral motion control for autonomous vehicle at driving limits. *Control Engineering Practice*, 76, 41–53.
- Kolås, S., Foss, B., and Schei, T. (2009). Constrained nonlinear state estimation based on the UKF approach. *Computers & Chemical Engineering*, 33(8), 1386–1401.
- Laurense, V.A., Goh, J.Y., and Gerdes, J.C. (2017). Path-tracking for autonomous vehicles at the limit of friction. In *2017 American Control Conference*, 5586–5591.
- Liu, J., Jayakumar, P., Stein, J.L., and Ersal, T. (2016). A study on model fidelity for model predictive control-based obstacle avoidance in high-speed autonomous ground vehicles. *Vehicle System Dynamics*, 54(11), 1629–1650.
- Liu, J., Jayakumar, P., Stein, J.L., and Ersal, T. (2017). Combined speed and steering control in high speed autonomous ground vehicles for obstacle avoidance using model predictive control. *IEEE Transactions on Vehicular Technology*, 66(10), 8746–8763.
- Liu, J., Jayakumar, P., Stein, J.L., and Ersal, T. (2019). Improving the robustness of an MPC-based obstacle avoidance algorithm to parametric uncertainty using worst-case scenarios. *Vehicle System Dynamics*, 57(6), 874–913.
- Pacejka, H.B. (2006). *Tyre and Vehicle Dynamics*. Butterworth-Heinemann.
- Ryu, J., Rossetter, E.J., and Gerdes, J.C. (2002). Vehicle Sideslip and Roll Parameter Estimation using GPS. In *International Symposium on Advanced Vehicle Control*, 373–380. Hiroshima, Japan.
- Schwarting, W., Alonso-Mora, J., Paull, L., Karaman, S., and Rus, D. (2017). Safe nonlinear trajectory generation for parallel autonomy with a dynamic vehicle model. *IEEE Transactions on Intelligent Transportation Systems*, 19(9), 2994–3008.
- Shim, T. and Ghike, C. (2007). Understanding the limitations of different vehicle models for roll dynamics studies. *Vehicle System Dynamics*, 45(3), 191–216.
- Wächter, A. and Biegler, L.T. (2006). On the implementation of an interior-point filter line-search algorithm for large-scale nonlinear programming. *Mathematical Programming*, 106(1), 25–57.
- Wan, E. and Van Der Merwe, R. (2000). The unscented Kalman filter for nonlinear estimation. In *IEEE Adaptive Systems for Signal Processing, Communications, and Control Symposium*, 153–158.
- Wurts, J., Stein, J.L., and Ersal, T. (2018). Collision imminent steering using nonlinear model predictive control. In *2018 Annual American Control Conference*, 4772–4777.
- Wurts, J., Stein, J.L., and Ersal, T. (2019). Minimum slip collision imminent steering in curved roads using nonlinear model predictive control. In *2019 Annual American Control Conference*, 3975–3980.